

1 **Title**

2 Drumming motor sequence training induces apparent myelin remodelling in
3 Huntington's disease: a longitudinal diffusion MRI and quantitative magnetization
4 transfer study

5

6 **Authors**

7 Chiara Casella^{1*}, Jose Bourbon-Teles^{1*}, Sonya Bells², Elizabeth Coulthard³, Greg D.
8 Parker¹, Anne Rosser^{4,6}, Derek K. Jones^{1,5}, Claudia Metzler-Baddeley¹

9 *These authors share first authorship

10

11 **Affiliations**

12 ¹ Cardiff University Brain Research Imaging Centre (CUBRIC), School of Psychology,
13 Cardiff University, Maindy Road, Cardiff, CF 24 4HQ, UK ² The Hospital for Sick
14 Children, Neurosciences and Mental Health, Toronto, M5G 1X8, Canada; ³ Clinical
15 Neurosciences, University of Bristol, Bristol, BS10 5NB, UK, ⁴ School of Biosciences,
16 Cardiff University, Museum Avenue, Cardiff, CF10 3AX, UK. ⁵
17 Mary MacKillop Institute for Health Research, Australian Catholic University,
18 Melbourne, Victoria 3065, Australia. ⁶ Department of Neurology and Psychological
19 Medicine, Hayden Ellis Building, Maindy Rd, CF24 4HQ

20

21 **Running title**

22 Training-associated myelin-remodelling in HD.

23

24 **Corresponding author**

25 Chiara Casella, CUBRIC, Maindy Road, Cardiff CF24 4 HQ, CasellaC@cardiff.ac.uk.

26 **1. Abstract**

27 **Background:** Impaired myelination may contribute to Huntington's disease (HD)
28 pathogenesis. **Objective:** This study assessed differences in white matter (WM)
29 microstructure between HD patients and controls, and tested whether drumming
30 training stimulates WM remodelling in HD. Furthermore, it examined whether training-
31 induced microstructural changes are related to improvements in motor and cognitive
32 function. **Methods:** Participants undertook two months of drumming exercises.
33 Working memory and executive function were assessed before and post-training.
34 Changes in WM microstructure were investigated with diffusion tensor magnetic
35 resonance imaging (DT-MRI)-based metrics, the restricted diffusion signal fraction (Fr)
36 from the composite hindered and restricted model of diffusion (CHARMED) and the
37 macromolecular proton fraction (MPF) from quantitative magnetization transfer (qMT)
38 imaging. WM pathways linking putamen and supplementary motor areas (SMA-
39 Putamen), and three segments of the corpus callosum (CCI, CCII, CCIII) were studied
40 using deterministic tractography. Baseline MPF differences between patients and
41 controls were assessed with tract-based spatial statistics (TBSS). **Results:** MPF was
42 reduced in the mid-section of the CC in HD subjects at baseline, while a significantly
43 greater change in MPF was detected in HD patients relative to controls in the CCII,
44 CCIII, and the right SMA-putamen post-training. Further, although patients improved
45 their drumming and executive function performance, such improvements did not
46 correlate with microstructural changes. Increased MPF suggests training-induced
47 myelin changes in HD. **Conclusions:** Though only preliminary and based on a small
48 sample size, these results suggest that tailored behavioural stimulation may lead to
49 neural benefits in early HD, that could be exploited for delaying disease progression.

50

51 **Key words**

52 Huntington's disease, drumming training, white matter, myelin, diffusion MRI

53

54 **2. Introduction**

55 **2.1 The Pathology of Huntington's disease**

56 Huntington's disease (HD) is a genetic, neurodegenerative disorder caused by
57 an expansion of the CAG repeat within the *huntingtin* gene, leading to debilitating
58 cognitive, psychiatric, and motor symptoms. In addition to striatal grey matter (GM)
59 degeneration [1], HD pathology has been linked to white matter (WM) changes [2–9].
60 Additionally, an increasing body of research suggests that myelin-associated
61 biological processes at the cellular and molecular level contribute to WM abnormalities
62 [10–15]. Myelin is a multi-layered membrane sheath wrapping axons and is produced
63 by oligodendrocytes. Axon myelination is vital during brain development and critical
64 for healthy brain function [16]. Oligodendrocyte/myelin dysfunction can slow down or
65 stop otherwise fast axonal transport, which in turn can result in synaptic loss and
66 eventually axonal degeneration [17].

67

68 **2.2 Interventions and Brain Plasticity**

69 As HD is caused by a single-gene, it is an ideal model to study
70 neurodegeneration as a whole, and test for possible beneficial interventions that can
71 slow or suppress disease onset. Despite this, no disease-modifying treatment is
72 approved for patients with HD at present. Recent developments in gene therapy have
73 generated much excitement. However, these have yet to be proved to lead to
74 measurable changes in disease progression [18]. Furthermore, a number of questions
75 linger, for example on the relative strength of different approaches and the possible

76 side effects of each therapy [19]. Importantly, these treatments aim to modify and not
77 cure the disease, and while symptomatic therapies for HD are present, and are used
78 for treating chorea and some of the psychiatric symptoms, their effectiveness varies
79 between patients and may lead to clinically significant side-effects [18]. This stresses
80 the need to develop better symptomatic therapies to aid patients and manage HD
81 symptoms.

82 Environmental stimulation and behavioural interventions may have the potential to
83 reduce disease progression and delay disease onset [20–22]. Furthermore, previous
84 studies have detected training-related changes in the WM of both healthy controls
85 [23,24] and patients, including subjects with HD [25]. For example, DT MRI studies
86 have shown microstructural WM changes following balance training in healthy [24] and
87 traumatic brain injury young adults [26]. Other imaging studies have shown DT MRI
88 changes as a result of juggling [27], abacus training [28], extensive piano practice
89 [29,30], working memory training [31], reasoning training [32], and meditation training
90 [33].

91 Converging evidence implicates myelin plasticity as one of the routes by which
92 experience shapes brain structure and function [27,34–38]. Plastic changes in
93 myelination may be implicated in early adaptation and longer-term consolidation and
94 improvement in motor tasks [39–42]. Changes in myelin-producing oligodendrocytes
95 and in GM and WM microstructure have been reported within the first hours of skill
96 acquisition [43,44], implying that experience can be quickly translated into adaptive
97 changes in the brain.

98 This study assessed whether two months of drumming training, involving
99 practising drumming patterns in ascending order of difficulty, could trigger WM
100 microstructural changes, and potentially myelin remodelling, in individuals with HD.

101 Specifically, we hypothesised that changes in *microstructural* metrics would be more
102 marked in patients than in healthy subjects, based on reports of larger training-
103 associated changes in structural MRI metrics in patient populations than in healthy
104 controls [34].

105 The drumming intervention was designed to target cognitive and motor
106 functions known to be mediated by cortico-basal ganglia loops. More specifically the
107 training focused on the learning of novel motor sequences and their rhythm and timing,
108 engaging executive processes known to be impaired in HD [45]. These included
109 focused attention (e.g. paying attention to the drumming sequence), multi-tasking
110 attention (e.g. listening and movement execution), movement-switching (e.g.
111 switching between dominant and non-dominant hand) and response speed [25]. At the
112 anatomical level, attention and executive functions rely on cortico-basal ganglia loops
113 involving the striatum, which also plays a fundamental role in motor control and motor
114 learning [46,47]. This shared reliance on overlapping cortico-basal ganglia networks
115 may contribute to the beneficial effects of physical exercise on executive functioning
116 in healthy older adults [48], and in patients with Parkinson's disease [49]. Additionally,
117 in a previous pilot study assessing the feasibility of the present drumming training, we
118 observed WM changes and improvements in executive functions in HD patients
119 following the intervention [25].

120 Previous WM plasticity neuroimaging studies [27,50] have predominantly
121 employed indices from diffusion tensor MRI (DT-MRI) [51]. However, while sensitive,
122 such measures are not specific to changes in specific sub-compartments of WM
123 microstructure, challenging the interpretation of any observed change in DT-MRI
124 indices [52,53]. To improve compartmental specificity beyond DT-MRI, the present
125 study explored changes in the macromolecular proton fraction (MPF) from quantitative

126 magnetization transfer (qMT) [54] imaging and the restricted diffusion signal fraction
127 (Fr) from the composite hindered and restricted model of diffusion (CHARMED) [55].
128 Fractional anisotropy (FA) and radial diffusivity (RD) from DT-MRI [51] were included
129 for comparability with previous training studies [27,56,57].

130 The MPF has been proposed as a proxy MRI marker of myelin [58].
131 Accordingly, histology studies show that this measure reflects demyelination
132 accurately in Shiverer mice [59], is sensitive to de-myelination in multiple sclerosis
133 patients [60] and reflects WM myelin content in post-mortem studies of multiple
134 sclerosis brains [61]. Fr, on the other hand, represents the fraction of signal-
135 attenuation that can be attributed to restricted diffusion, which is presumed to be
136 predominantly intra-axonal, and therefore provides a proxy measure of axonal density
137 [62].

138 Training effects were investigated in WM pathways linking the putamen and the
139 supplementary motor area (SMA-Putamen), and within three segments of the corpus
140 callosum (CCI, CCII, CCIII). The SMA has efferent and afferent projections to the
141 primary motor cortex and is involved in movement execution, and previous work has
142 reported altered DT-MRI metrics in the putamen-motor tracts of symptomatic HD
143 patients [63]. The anterior and anterior-mid sections of the corpus callosum contain
144 fibres connecting the motor, premotor and supplementary motor areas in each
145 hemisphere [64]. Previous work has demonstrated a thinning of the corpus callosum
146 in post-mortem HD brains [65], altered callosal DT-MRI metrics in both pre-
147 symptomatic and symptomatic HD patients [66,67], and a correlation between these
148 metrics and performance on motor function tests [68]. Given previous reports of an
149 effect of motor learning on myelin plasticity [38], we expected changes following
150 training to be more marked in MPF, as compared to the other non-myelin sensitive

151 metrics assessed in this study. We also investigated the relationship between training-
152 associated changes in MRI measures, and changes in drumming performance and
153 cognitive/executive function. Finally, as previous evidence has shown widespread
154 reductions in MPF in premanifest and manifest HD patients [69], we used tract-based
155 spatial statistics (TBSS) [70] to investigate patient-control differences in MPF before
156 training, across the whole brain; this aided the interpretation of the post-training
157 microstructure changes we detected.

158

159 **3. Materials and Methods**

160 **3.1 Participants**

161 The study was approved by the local National Health Service (NHS) Research
162 Ethics Committee (Wales REC 1 13/WA/0326) and all participants provided written
163 informed consent. All subjects were drumming novices and none had taken part in our
164 previously-reported pilot study [25]. Fifteen HD patients were recruited from HD clinics
165 in Cardiff and Bristol. Genetic testing confirmed the presence of the mutant huntingtin
166 allele. Thirteen age, sex, and education-matched healthy controls were recruited from
167 the School of Psychology community panel at Cardiff University and from patients'
168 spouses, carers or family members. The inclusion criteria were the following: no
169 history of head injury, stroke, cerebral haemorrhages or any other neurological
170 condition; eligible for MRI scanning; stable medication for at least four weeks prior to
171 the study.

172 Of the recruited sample, two patients were not MRI compatible, four withdrew
173 during the study and one patient's MRI data had to be excluded due to excessive
174 motion. Therefore, while drumming performance and cognitive data from 11 patients
175 were assessed, only 8 patients had a complete MRI dataset. One control participant

176 was excluded due to an incidental MRI finding, two participants dropped out of the
177 study and a fourth participant was not eligible for MRI. In total, we assessed drumming
178 and cognitive tests performance in 8 controls, while MRI data from nine controls were
179 available for analyses. Table 1 summarizes patients demographic and background
180 clinical characteristics. Most patients were at early disease stages, however two were
181 more advanced, as shown by their Total Motor Score (TMS; 69 and 40, respectively)
182 and Functional Assessment Score (FAS; 18 and 17, respectively). Table 2
183 summarizes demographic variables and performance in the Montreal Cognitive
184 Assessment (MoCA) [71] and in the revised National Adult Reading Test (NART-R)
185 (Nelson, 1991) for patients and controls. While the groups did not differ significantly in
186 age, controls were on average slightly older, performed significantly better on the
187 MoCA, and had a significantly higher NART-IQ than patients.

188

189 ***3.2 Training intervention: Drumming-based rhythm exercises***

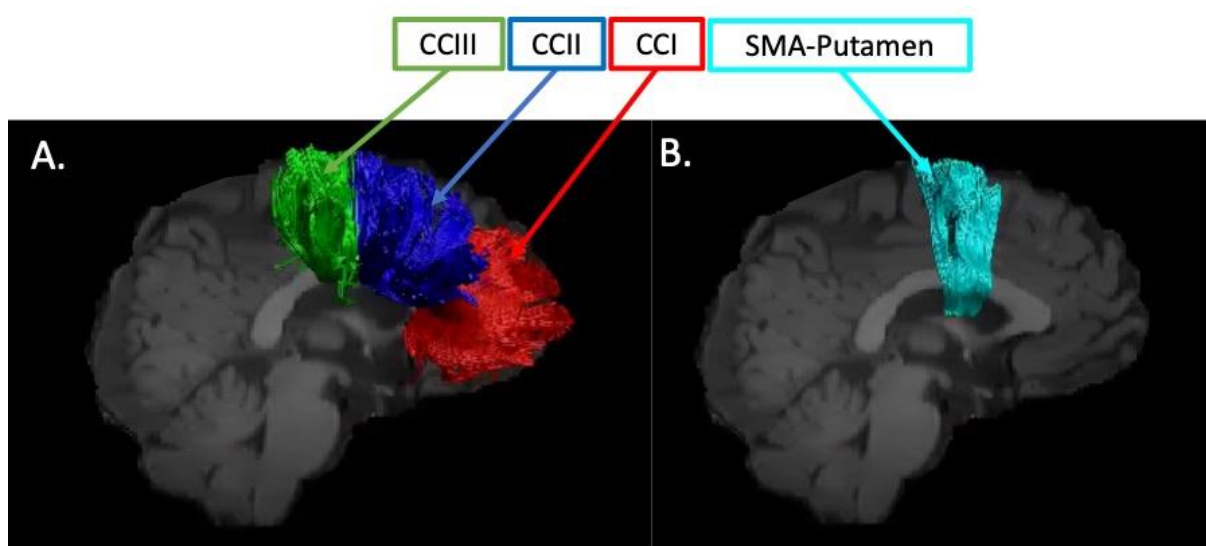
190 The rhythm exercise and drumming training previously described in [25] was
191 applied. Participants were provided with twenty-two 15 min training sessions on CDs,
192 a pair of Bongo drums and a drumming diary and could practise at home. They were
193 asked to exercise for 15 min per day, 5 times per week, for 2 months and to record the
194 date and time of each exercise in their diary. Each training session introduced a
195 drumming pattern based on one of the following rhythms: Brazilian samba, Spanish
196 rumba, West-African kuku and Cuban son. After a brief warm up, trainees were
197 encouraged to drum along with the instructor, initially with each hand separately and
198 then with both hands alternating, starting with the dominant hand first and then
199 reversing the order of the hands. The first exercises were based on very simple, slow,

200 and regular patterns but the level of complexity and speed increased over the training
201 sessions.

202 Importantly, each individual progressed through the training adaptively at their
203 own pace i.e., as long as they exercised for the specified time, they could repeat each
204 session as often as they felt necessary to master it. To maintain engagement and
205 motivation, the training incorporated pieces of music based on rhythms participants
206 had learned and could drum along to. The researcher (JBT) supervised the first
207 training sessions and then remained in regular telephone contact (at least once a
208 week) with each participant throughout the intervention. Whenever possible, carers
209 and/or spouses were involved in the study to support the training. Control participants
210 started with Session 3 since the first two exercises were built on a very low level of
211 complexity, with slow, regular patterns of movement required. Patients, on the other
212 hand, started with simpler exercises, but could progress to the following sessions
213 whenever they felt comfortable.

214

215



216

217 **Figure 1.**

218

219

220 **3.3 Drumming assessment**

221 Progress in drumming ability was assessed by digitally recording participants'
222 drumming performance for three patterns of ascending levels of difficulty (easy,
223 medium and hard), which were not part of the training sessions, at baseline and after
224 the training. Each recording was judged by an independent rater, blind to group and
225 time, according to an adopted version of the Trinity College London marking criteria
226 for percussion (2016) (www.trinitycollege.com).

227

228 **3.4 Cognitive assessments**

229 Different aspects of cognition and executive function were assessed before and
230 after the training as previously described [25]. Multi-tasking was assessed with a dual
231 task requiring simultaneous box crossing and digit sequences repetition [73]. Attention
232 switching was assessed with the trails test (VT) requiring the verbal generation of letter
233 and digit sequences in alternate order relative to a baseline condition of generating
234 letter or digit sequences only (69). Distractor suppression was tested with the Stroop
235 task involving the naming of incongruent ink colours of colour words. Verbal and
236 category fluency were tested using the letter cues "F", "A", "S" and "M", "C", "R" as well
237 as the categories of "animals" and "boys' names" and "supermarket items" and "girls'
238 names" respectively [74]. In total, we assessed 7 outcome variables, and percentage
239 change scores in performance were computed for each of these variables (Table 3).

240

241 **3.5 MRI data acquisition**

242 MRI data were acquired on a 3 Tesla General Electric HDx MRI system (GE
243 Medical Systems, Milwaukee) using an eight channel receive-only head RF coil at the
244 Cardiff University Brain Research Imaging Centre (CUBRIC). The MRI protocol
245 comprised the following images sequences: a high-resolution fast spoiled gradient
246 echo (FSPGR) T₁-weighted (T₁-w) sequence for registration; a diffusion-weighted
247 spin-echo echo-planar sequence (SE\EPI) with 60 uniformly distributed directions
248 ($b = 1200 \text{ s/mm}^2$), according to an optimized gradient vector scheme [75]; a
249 CHARMED acquisition with 45 gradient orientations distributed on 8 shells (maximum
250 b -value = 8700 s/mm^2) [55]; and a 3D MT-weighted fast spoiled gradient recalled-echo
251 (FSPGR) sequence [76]. The acquisition parameters of all scan sequences are
252 reported in Table 4. Diffusion data acquisition was peripherally gated to the cardiac
253 cycle. The off-resonance irradiation frequencies (Θ) and their corresponding
254 saturation pulse amplitude (ΔSAT) for the 11 Magnetization transfer (MT) weighted
255 images were optimized using Cramer-Rao lower bound optimization [76].

256

257 **3.6 MRI data processing**

258 The diffusion-weighted data were corrected for distortions induced by the
259 diffusion-weighted gradients, artefacts due to head motion and EPI-induced
260 geometrical distortions by registering each image volume to the T₁-w anatomical
261 images [77], with appropriate reorientation of the encoding vectors [78], all done in
262 ExploreDTI (Version 4.8.3) [79]. A two-compartment model was fitted to derive maps
263 of FA and RD in each voxel [80]. CHARMED data were corrected for motion and
264 distortion artefacts according to the extrapolation method of [81] The number of
265 distinct fiber populations (1, 2, or 3) in each voxel was obtained using a model selection
266 approach [52], and Fr was calculated per voxel with an in-house software [52] coded

267 in MATLAB (The MathWorks, Natick, MA). MT-weighted SPGR volumes for each
268 participant were co-registered to the MT-volume with the most contrast using an affine
269 (12 degrees of freedom, mutual information) registration to correct for inter-scan
270 motion using Elastix [82]. The 11 MT-weighted SPGR images and T₁ map were
271 modelled by the two pool Ramani's pulsed MT approximation [83,84], which included
272 corrections for amplitude of B₀ field inhomogeneities. This approximation provided
273 MPF maps, which were nonlinearly warped to the T₁-w images using the MT-volume
274 with the most contrast as a reference using Elastix (normalized mutual information
275 cost function) [82].

276

277 **3.7 Deterministic Tractography**

278 Training-related changes in FA, RD, Fr, and MPF were quantified using a
279 tractography approach in pathways interconnecting the putamen and the
280 supplementary motor area bilaterally (SMA-Putamen), and within three segments of
281 the corpus callosum (CCI, CCII and CCIII) [64] (Figure 1).

282 Whole brain tractography was performed for each participant in their native
283 space using the damped Richardson-Lucy algorithm [85], which allows the recovery
284 of multiple fiber orientations within each voxel including those affected by partial
285 volume. The tracking algorithm estimated peaks in the fiber orientation density function
286 (fODF) by selecting seed points at the vertices of a 2x2x2 mm grid superimposed over
287 the image and propagated in 0.5-mm steps along these axes re-estimating the fODF
288 peaks at each new location [86]. Tracks were terminated if the fODF threshold fell
289 below 0.05 or the direction of pathways changed through an angle greater than 45°
290 between successive 0.5 mm steps. This procedure was then repeated by tracking in
291 the opposite direction from the initial seed-points.

292 The WM tracts of interest were extracted from the whole-brain tractograms by
293 applying way-point regions of interest (ROI) [87]. These were drawn manually by one
294 operator (JBT) blind to the identity of each dataset on color-coded fiber orientation
295 maps in native space guided by the following anatomical landmark protocols (Figure
296 2).

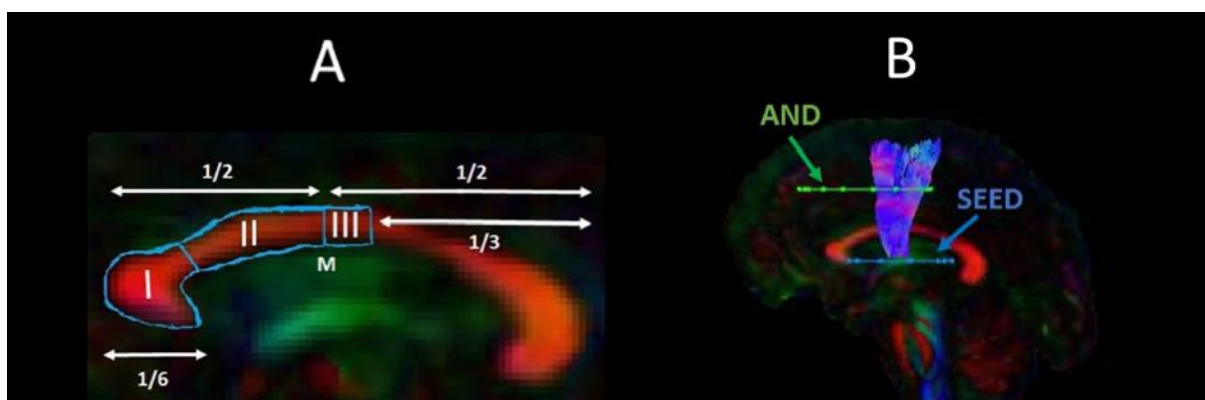
297 3.7.1 Corpus callosum

298 Reconstruction of the CC segments followed the protocol of Hofer and Frahm
299 [64] as illustrated in Figure 2A. Segment reconstructions were visually inspected and,
300 if necessary, additional gates were placed to exclude streamlines inconsistent with the
301 known anatomy of the CC.

302 3.7.2 SMA-putamen pathway

303 One axial way-point ROI was placed around the putamen and one axial ROI
304 around the supplementary motor cortex [88] (Figure 2B). A way-point gate to exclude
305 fibres projecting to the brain stem was placed inferior to the putamen.

306
307



308
309 **Figure 2.**

310
311

312 **3.8 Statistical analyses**

313 Statistical analyses were carried out in R Statistical Software (Foundation for
314 Statistical Computing, Vienna, Austria).

315 3.8.1 Assessment of training effects on drumming performance

316 Improvements in drumming performance were analysed with a two-way mixed
317 analysis of variance (ANOVA) testing for the effects of group (HD/controls), time of
318 assessment (before/after the training) and group by time interaction effects. We also
319 confirmed detected effects to the ones obtained by running a robust mixed ANOVA,
320 using the bwtrim R function from the WRS2 package [89]. This implements robust
321 methods for statistical estimation and therefore provides a good option to deal with
322 data presenting small sample sizes, skewed distributions and outliers [90]. Significant
323 effects were further explored with post-hoc paired and independent t-tests. The
324 reliability of the post-hoc analyses was assessed with bootstrap analysis based on
325 1000 samples and the 95% confidence interval (CI) of the mean difference is provided
326 for each significant comparison.

327 3.8.2 Assessment of group differences in the effect of training on cognitive 328 performance

329 Performance measures in executive function tasks have been shown to share
330 underlying cognitive structures [91]. Therefore, PCA was employed to reduce the
331 complexity of the cognitive data and hence the problem of multiple comparisons as
332 well as to increase experimental power. PCA was run on change scores for all
333 participants across both groups. Due to the relatively small sample size, we first
334 confirmed with the Kaiser-Meyer-Olkin (KMO) test that our data was suited for PCA.
335 Subsequently, we followed guidelines to limit the number of extracted components
336 [92,93], as follows: first, we employed the Kaiser criterion of including all components

337 with an eigenvalue greater than 1; second, we inspected the Cattell scree plot [94] to
338 identify the minimal number of components that accounted for most variability in the
339 data; third, we assessed each component's interpretability. A PCA procedure with
340 orthogonal Varimax rotation of the component matrix was used. Loadings that
341 exceeded a value of 0.5 were considered as significant.

342 Next, we assessed group differences in the component scores with permutation
343 analyses, to understand whether the training had differentially affected HD patients as
344 compared to controls. Permutation testing relies only on minimal assumptions and can
345 therefore be applied when the assumptions of a parametric approach are untenable
346 such as in the case of small sample sizes. Significant group differences were tested
347 using 5,000 permutations and the effect sizes of significant differences were assessed
348 with Cohen's d [95]. Multiple comparison correction was based on a 5% false
349 discovery rate (FDR) using the Benjamini-Hochberg procedure [96].

350 3.8.3 Training effects on WM microstructure

351 Median measures of FA, RD, Fr and MPF were derived for each of the
352 reconstructed tracts in ExploreDTI [79]. A percentage change score in these measures
353 between baseline and post-training was calculated in each tract (CCI, CCII, CCIII, left
354 and right SMA-Putamen).

355 Previous research has shown that variation in the microstructural properties of
356 WM may represent a global effect, rather than being specific to individual tracts, and
357 that WM measures are highly correlated across WM areas [56,97,98]. Therefore, we
358 inspected the inter-tract correlation for each of microstructural metric and found that
359 MPF values were highly correlated, whereas this was not true for the other metrics
360 (Figure 3). Hence, percentage change scores in MPF across the different tracts were
361 transformed with PCA to extract meaningful anatomical properties, following the

362 procedure described above for the PCA of cognitive change scores. PC scores for
363 each participant were then used as dependent variables in a permutation-based
364 analysis using 5,000 permutations to assess group differences in training associated
365 changes in MPF. Finally, as a post-hoc exploration, we looked for between-groups
366 differences in MPF changes in the individual tracts using 5000 permutations.

367 Training-associated changes in FA, Fr and RD were investigated with
368 permutation analyses separately for each tract. Significant group differences in these
369 measures were tested using 5,000 permutations. Multiple comparison correction was
370 based on a 5% FDR using the Benjamini-Hochberg procedure [96]. Cohen's d [95]
371 was used to assess the effect size for those changes found to be significant.

372 3.8.4 Training effects on WM microstructure

373 TBSS [70] was carried out to investigate baseline differences in MPF between
374 HD subjects and healthy controls, , to gain a better insight into differences in training-
375 associated changes. To produce significance maps, a voxel-wise analysis was
376 performed on the MPF projected 4D data for all voxels with FA ≥ 0.20 to exclude
377 peripheral tracts where significant inter-subject variability exists. Inference based on
378 permutations (5,000 permutations) and threshold-free-cluster-enhancement was
379 used. The significance level was set at $p < 0.05$ and corrected by multiple comparisons
380 (family-wise error, FWE).

381 3.8.5 Relationship between changes in MRI measures and changes in drumming and 382 cognitive performance

383 We computed percentage change scores for the drumming performance, in the
384 same way cognitive change scores were calculated. Scores were computed for the
385 easy test pattern in patients and for the medium test pattern in controls, as these
386 training patterns showed a significant improvement in the two groups, respectively.

387 Spearman correlation coefficients were calculated between drumming and cognitive
388 performance, and microstructural components that showed significant group
389 differences, to assess whether microstructural changes were related to any drumming
390 and/or cognitive benefits of the training.

391 3.8.6 Exploration of the possible confounding effects of differences in training- 392 compliance and IQ

393 We examined the training diaries of each participant to assess compliance with
394 training. Each session was marked as completed if the whole 15 minute session had
395 been carried out. Each participant was assigned a score representing the number of
396 training sessions they performed (e.g. a score of 40 if 40 sessions had been carried
397 out). We then assessed group differences with permutation analyses, to test whether
398 there was a significant difference in the amount of training sessions carried out by the
399 groups, and hence understand whether this variable had to be accounted for in the
400 analysis. Significant group differences were tested using 5,000 permutations.

401 Finally, as there was a significant difference in IQ between patients and controls
402 (Table 2), we investigated whether any training-associated change might be due to
403 differences in premorbid intelligence. The sample size of this experiment was very
404 small, and therefore it was not possible to perform a multiple regression or an analysis
405 of covariance (ANCOVA), to understand the possible influence of IQ as confounding
406 variable. Accordingly, the statistical power to establish the incremental validity of a
407 covariate in explaining an outcome has been shown to be extremely low, and therefore
408 to require large sample sizes [99]. As a potential solution to this issue, we instead
409 performed separate non-parametric Spearman correlation analyses between NART-
410 IQ scores (as this test showed the largest difference between groups), and MRI and
411 cognitive measures showing significant training effects; this allowed us to gain some

412 insight into whether there was a significant association between premorbid intelligence
413 and training-associated changes.

414

415

416 **4. Results**

417 **4.1 Training effects on drumming performance**

418 The mixed ANOVA of drumming performance for the easy and medium test
419 pattern showed a significant effect of group [easy: $F(1,17) = 22.3$, $p < 0.001$; medium:
420 $F(1,17) = 13.1$, $p = 0.002$] and time [easy: $F(1,17) = 12.83$, $p = 0.004$; medium: $F(1,17)$
421 $= 13.4$, $p = 0.002$] but no interaction (easy: $p = 0.8$; medium: $p = 0.3$). For the hard test
422 pattern there was only a significant effect of group [$F(1,17) = 9.95$, $p = 0.006$] but not
423 of time ($p = 0.1$) and there was no interaction ($p = 0.4$). Results from the robust mixed
424 ANOVA were largely consistent with the above. Specifically, the easy and medium test
425 patterns showed a significant effect of group (easy: $p = 0.002$; medium: $p = 0.02$) and
426 time (easy: $p = 0.04$; medium: $p = 0.049$) but no interaction (easy: $p = 0.45$; medium:
427 $p = 0.69$). The hard test pattern showed a significant effect of group ($p = 0.02$) but not
428 of time ($p = 0.22$) and no interaction ($p = 0.8$). Figure 4 summarises the average
429 drumming performance per group and time point. Overall patients' drumming
430 performance was poorer than controls. Patients improved their drumming
431 performance significantly for the easy pattern [$t(10) = 2.7$, $p = 0.02$; 95% CI of mean
432 difference: 1.5 – 7.8] and controls for the medium pattern [$t(7) = 3.8$, $p = 0.01$; 95% CI
433 of mean difference: 2.8 – 8.5].

434

435 **4.2 Group differences in the effect of training on cognitive performance**

436 Three components, accounting for 79% of the variance in performance
437 improvement in the cognitive benchmark tests, were extracted. The first component
438 loaded highly on performance changes in the dual task (total number of boxes
439 identified under dual task condition), the Stroop task (Stroop interference score), and
440 the trails making task (Trail test switching). Since these variables all measure
441 executive functions including focused attention and distractor suppression, the first
442 component was labelled “executive” component. The second component loaded on
443 variables reflecting the ability to correctly recall digits sequences (i.e. number of
444 correct digits recalled under single and dual task condition) and was therefore labelled
445 “working memory capacity” component. Finally, the third extracted component loaded
446 highly on verbal and category fluency and was therefore labelled “fluency” component
447 (Table 5).

448 We tested whether the two groups differed in terms of post-training cognition
449 changes, by running permutation analyses on the individual scores for the three
450 extracted components. The two groups differed in the executive component ($t = -1.03$,
451 $p = 0.008$, FDR-corrected $p = 0.024$, $d = 1.15$). However, no significant group
452 differences were detected in the other two components (Working Memory capacity: t
453 $= -0.22$, $p = 0.3296$, FDR-corrected $p = 0.3296$; Fluency: $t = -0.39$, $p = 0.242$ FDR
454 corrected $p = 0.3296$).

455

456 **4.3 Training effects on WM microstructure**

457 Table 6 reports a summary of the training associated changes in FA, RD, Fr
458 and MPF, across the different tracts.

459 4.3.1 Training-associated group differences in FA

460 Permutation analyses of FA changes across the different tracts revealed no
461 significant differences between HD and control groups [CCI: $t = 1.22$, $p = 0.91$ (FDR-
462 corrected); CCII: $t = 2.65$, $p = 0.91$ (FDR-corrected); CCIII: $t = 0.325$, $p = 0.13$ (FDR-
463 corrected); right SMA-Putamen: $t = -9.54$, $p = 0.10$ (FDR-corrected); left SMA-
464 Putamen: $t = 5.16$, $p = 0.77$ (FDR-corrected).

465 4.3.2 Training-associated group differences in RD

466 There were no significant differences in RD changes following training
467 between HD patients and controls [CCI: $t = -0.48$, $p = 0.45$ (FDR-corrected); CCII: $t =$
468 -1.29 , $p = 0.45$ (FDM-corrected); CCIII: $t = -1.04$, $p = 0.45$ (FDR-corrected); right SMA-
469 Putamen, $t = 4.01$, $p = 0.81$ (FDR-corrected); left SMA-Putamen, $t = -3.68$, $p = 0.39$
470 (FDR-corrected).

471 4.3.3 Training-associated group differences in Fr

472 Permutation analyses of Fr changes across the different tracts revealed no
473 significant differences between HD and control groups [CCI: $t = 3.39$, $p = 0.82$ (FDR-
474 corrected; CCII: $t = -0.17$, $p = 0.82$ FDR-corrected; CCIII: $t = 3.08$, $p = 0.82$ (FDR-
475 corrected); right SMA-Putamen: $t = -5.24$, $p = 0.82$ (FDR-corrected); left SMA-
476 Putamen: $t = 1.05$, $p = 0.82$ (FDR-corrected)].

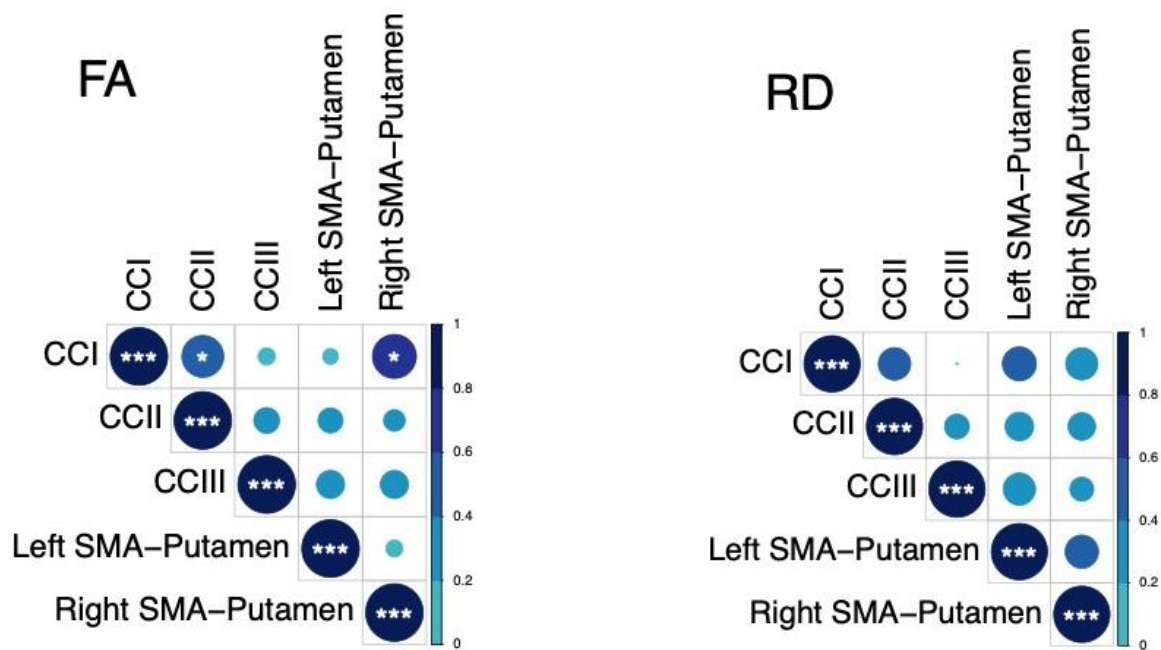
477 4.3.4 Training-associated group differences in MPF

478 PCA of change scores in MPF revealed one single component explaining
479 70.2% of the variance. This component presented high loadings from all the tracts
480 investigated. A significant group difference was found for the MPF change-score
481 component, indicating that HD patients presented significantly greater MPF changes
482 in response to training, as compared to controls [$t(14) = -1.743$, $n = 17$, $p = 0.03$, $d =$
483 1.796].

484 Finally, we found a significant difference in mean MPF change scores between
 485 the two groups for CCII [$t(14) = -20.72$, $p = 0.04$, $d = 0.93$], CCIII [$t(14) = -25.87$, $p =$
 486 0.04 , $d = 1.07$], and the right SMA-putamen pathway [$t(14) = -25.48$, $p = 0.04$, $d = 1.15$]
 487 after FDR correction, therefore indicating that there was a differential group effect of
 488 training on MPF within these tracts (Figure 5).

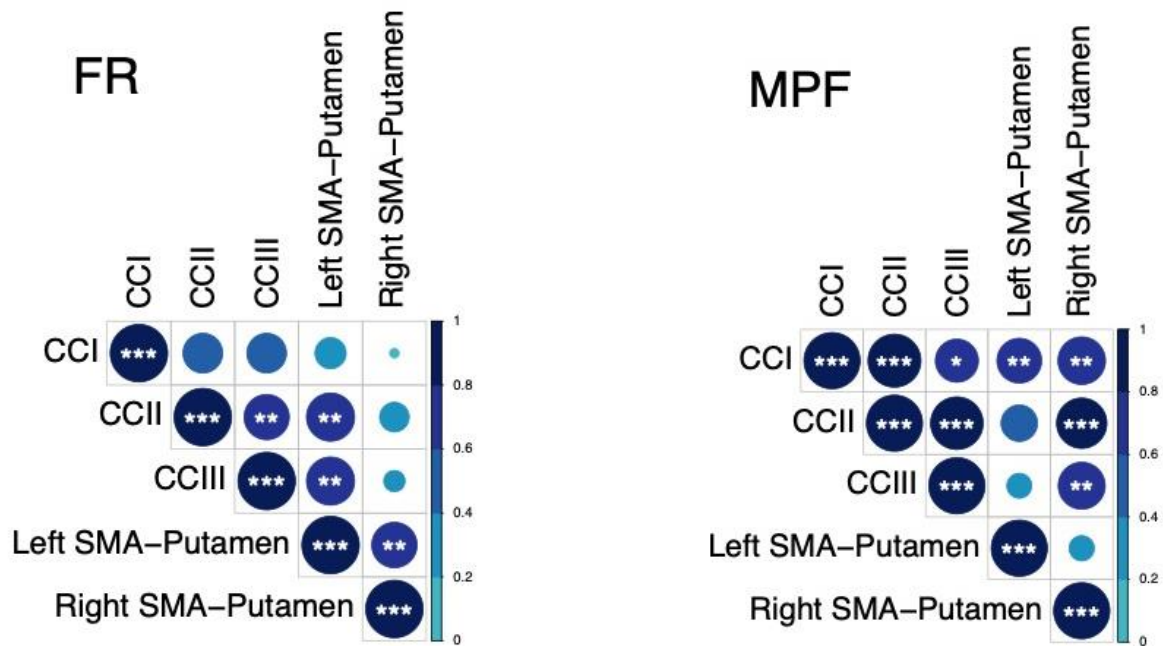
489

490



491

492



493

494 **Figure 3.**

495

496

497 **4.4 Relationship between training-associated changes in MRI measures, and**
 498 **changes in drumming and cognitive performance.**

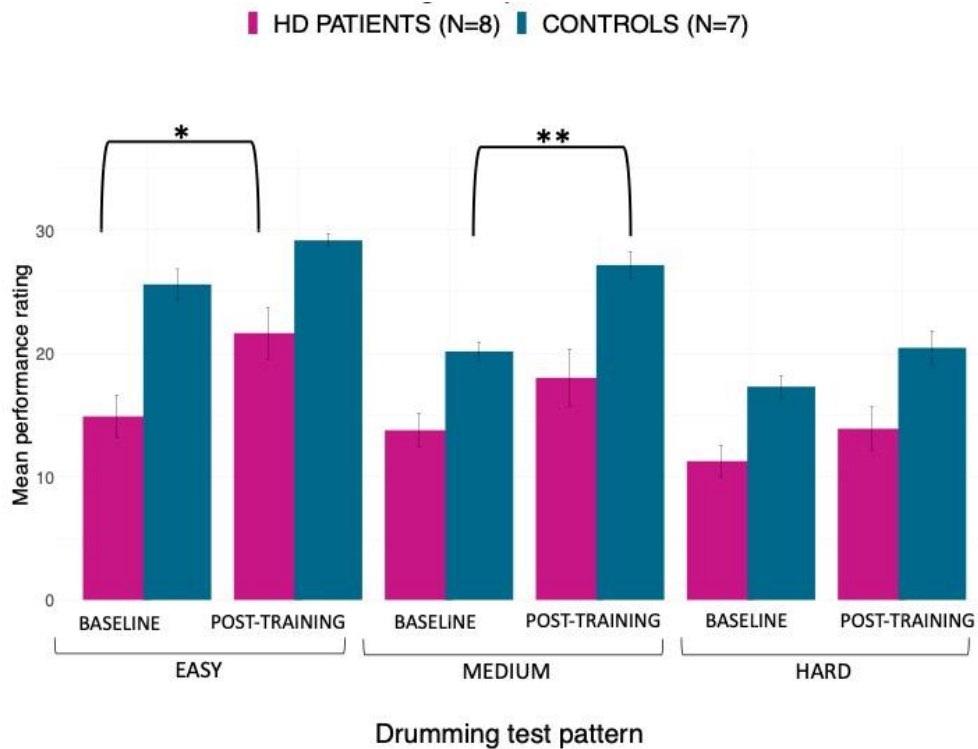
499 We did not find a significant association between the ‘MPF’ component scores
 500 and improvement in drumming performance (PC1: rho = -0.14, p > 0.05). Moreover,
 501 although no significant correlation was observed between the ‘Executive’ and the
 502 ‘MPF’ component scores, there was a positive trend (rho = .348, p = .171).

503

504 **4.5 Baseline differences in MPF**

505 Baseline MPF was reduced in the HD group compared to controls, in the
 506 midbody of the CC (t = 3.13, p = .05, FWE corrected). Figure 6 shows the areas with
 507 reduced MPF in HD patients, in blue.

508



509

510 **Figure 4.**

511

512

513 **4.6. Exploration of the possible confounding effects of differences in training-**
 514 **compliance and IQ**

515 The permutation analysis of training compliance revealed that there was not a
 516 significant difference in the number of training sessions between HD patients (mean =
 517 38.1, SD = 4.2) and healthy controls (mean = 39.6, SD = 1.2), $t = 1.45$, $p = 0.76$.
 518 Therefore, the total time spent training should not have influenced any training-
 519 associated change in microstructure and/or cognitive measures. Furthermore, we did
 520 not detect a significant association of participants' NART-IQ scores with 'MPF'
 521 component scores ($\rho = -0.4$, $p = 0.10$), nor with 'Executive' component scores (ρ
 522 = -0.34 , $p = 0.18$), suggesting that premorbid intelligence should not have had an
 523 influence on training-associated effects.

524

525 **5. Discussion**

526 Based on evidence that myelin impairment contributes to WM damage in HD
527 [3], and the suggestion that myelin plasticity underlies the learning of new motor skills
528 [27,38], the present study explored whether two months of drumming training would
529 result in changes in WM microstructure in HD patients. Specifically, we expected to
530 detect changes in MPF, as marker of WM myelin plasticity, in HD patients relative to
531 healthy controls.

532 Firstly, we demonstrated a behavioural effect of the training by showing a
533 significant improvement in drumming performance in patients (easy test pattern) and
534 controls (medium test pattern). We did not detect any group differences in training-
535 associated changes in the diffusion based indices of FA, RD and Fr. However, as
536 hypothesised, we found a group difference in training-induced changes in the MPF
537 PCA component. Specifically, HD patients showed significantly higher increases in
538 MPF relative to controls. Furthermore, through exploratory post-hoc investigations, we
539 detected significantly higher training-induced MPF changes within the CCII, CCIII and
540 the right SMA-putamen pathway between patients and controls. Additionally, TBSS
541 analysis of baseline differences in MPF suggested partial overlap of WM areas
542 showing significant MPF reductions at baseline with areas showing changes post-
543 training (i.e. CCII and CCIII).

544 MPF can be affected by inflammation [100] and in advanced HD it is likely that
545 inflammation goes hand-in-hand with myelin breakdown [101]. However, a recent CSF
546 biomarker study found no evidence of neuro-inflammation in early-manifest HD [102].
547 Furthermore, recent evidence shows that this measure may be inconsistent when
548 investigated in relatively small WM areas, presumably because of the effect of spatial
549 heterogeneity in myelin thickness [103]. Nevertheless, the within-subjects design

550 employed in the present study should have helped to minimise noise due to the spatial
551 inconsistency of this measure. Therefore, though preliminary and based on a small
552 sample size, these findings suggest that two months of drumming and rhythm
553 exercises may result in myelin remodelling in patients with early HD.

554 It is plausible that this group difference arose due to WM microstructural
555 differences between patients and controls before the training. Accordingly, the HD
556 group showed a significantly lower baseline MPF, consistent with lower myelin content
557 [3]. Furthermore, previous studies have reported that training-associated percentage
558 changes in MRI measures tend to be higher in patients than in healthy subjects [34].
559 One possibility is that in the healthy brain, neural networks may be optimally
560 myelinated, and further increasing myelin may not improve performance [104–106].
561 Hence, the MPF changes in patients relative to controls might depict mainly a ‘catch-
562 up effect’ to the better baseline status of the control group. However, disentangling the
563 impact of prior WM microstructural differences on microstructural plasticity during
564 learning is beyond the scope of the current work.

565 Notably, the behavioral effect of drumming training and cognition differed
566 between patients and controls. Patients improved in the easy drumming test pattern,
567 and controls improved in the medium test pattern. Furthermore, consistent with
568 evidence from our pilot study [25], patients showed increases in the executive function
569 components whilst control participants did not show improvements in their cognition.
570 Therefore, inter-group differences in microstructural changes might not only be due to
571 baseline WM microstructural differences, but also to a different behavioral effect of the
572 task between HD subjects and controls. For instance, control participants performed
573 close to ceiling in the easy test pattern, and as the training was tailored to patients’
574 needs, some of the earlier practice sessions may not have optimally challenged them.

575 The fact that the training seemed more taxing for patients than controls may also
576 explain why improvements in executive functions and changes in MPF were only
577 observed for the patients. Interestingly, baseline IQ was significantly different between
578 the two groups, and this might have had some influence on training performance and
579 on training-associated effects. Here, we failed to find an association between IQ
580 scores and changes in MRI and cognitive measures. However, future studies with
581 larger sample sizes might allow to utilize more advanced statistical approaches, such
582 as an ANCOVA, to better model the possible influence of premorbid IQ on training
583 effects, both at the neural and cognitive level.

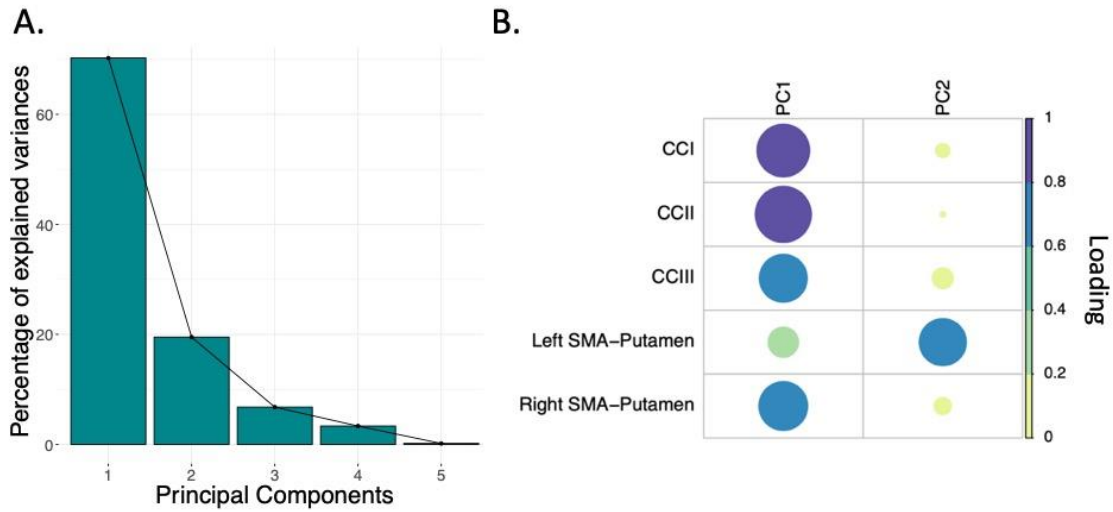
584 A critical question relevant to all training studies concerns the functional
585 significance of any observed neural changes. If, and to what degree adaptive
586 alterations in myelin content can facilitate behavioural change remains poorly
587 understood [105]. In the present study, no significant relationships between changes
588 in MRI measures and changes in drumming proficiency or performance in cognitive
589 tests were found. This might have been due to non-specific training-related neural
590 responses. Specifically, while the training exercise might have triggered changes in
591 brain structure, training-induced changes may not necessarily co-vary with
592 improvements in performance. Alternatively, it might be that the study was
593 insufficiently powered to detect brain-function correlations. The minimum sample size
594 required to detect a correlation was calculated to be 64 people ($\alpha = 0.05$; 80% power;
595 medium effect size; GPower 3 software). Therefore, these results need replication in
596 larger samples. A lack of correlation between structural and functional changes after
597 training has been reported in other studies (including well-powered studies) and may
598 suggest that these processes follow different time courses and/or may occur in
599 different brain regions [107].

600 It is important to note that our study did not include a non-intervention patient
601 group. Within the 12 month time period of this study it was not possible to recruit a
602 sufficiently large number of well-matched patient controls. Therefore, we cannot
603 disentangle the effects of the training on WM microstructure from HD-associated
604 pathological changes. However, given that HD is a progressive neurodegenerative
605 disease associated with demyelination [3], it is unlikely that increases in MPF observed
606 in the patient group were due to the disease itself. Finally, while the majority of training
607 studies assess brain structural changes between baseline and post-training [34],
608 presumably on account of cost and participant compliance, we suggest that acquiring
609 intermittent scans during the training period could have helped to better capture and
610 understand changes in WM microstructure observed in this study. Accordingly, future
611 studies might be able to provide greater insights into the complex nonlinear
612 relationships between structural changes and behaviour [108].

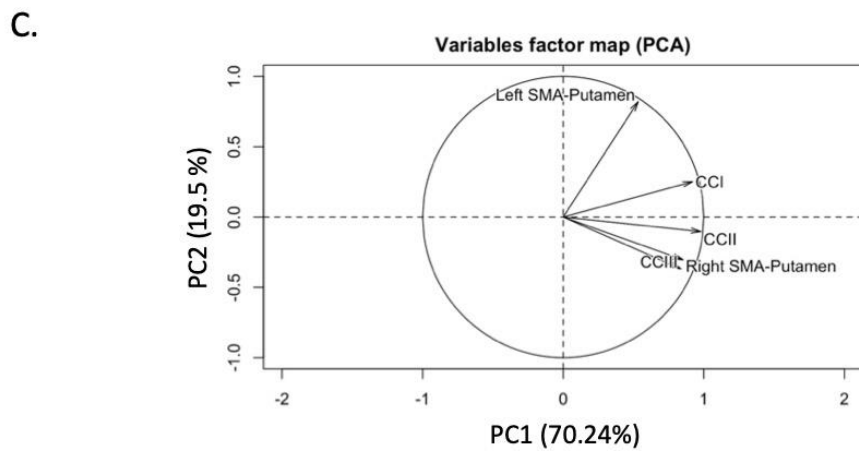
613 To conclude, we have demonstrated that two months of drumming and rhythm
614 exercises result in a significantly greater change in a proxy MRI measure of myelin in
615 patients with HD relative to healthy controls. Whilst the current results require
616 replication in a larger patient group with an appropriately matched patient control
617 group, they suggest that behavioural stimulation may result in neural benefits in HD
618 that could be exploited for future therapeutics aiming to delay disease progression.

619

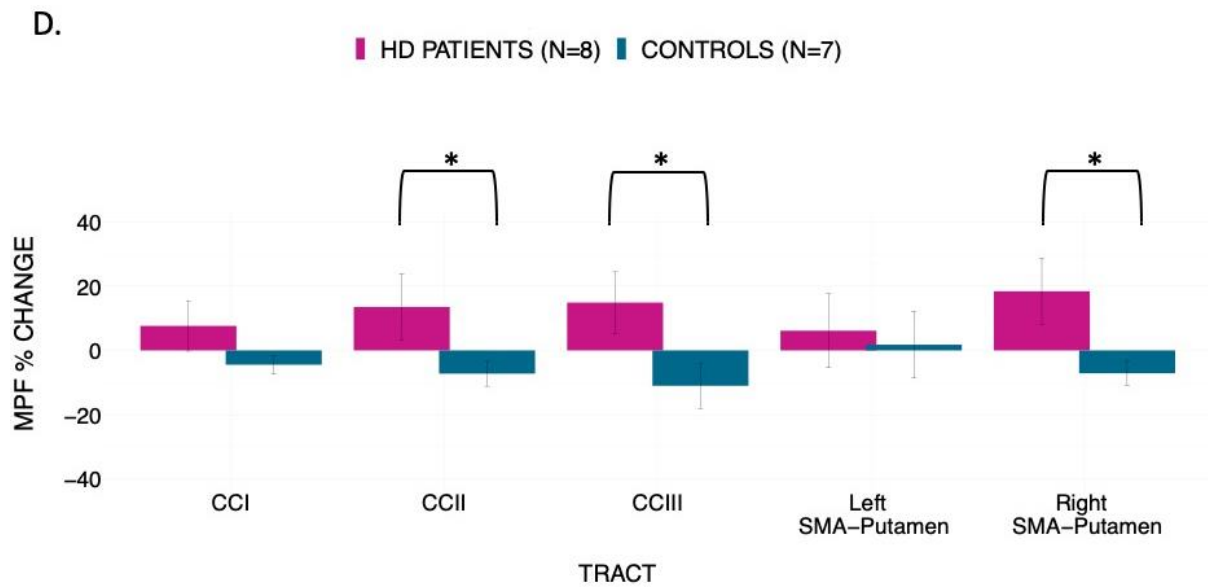
620



621



622

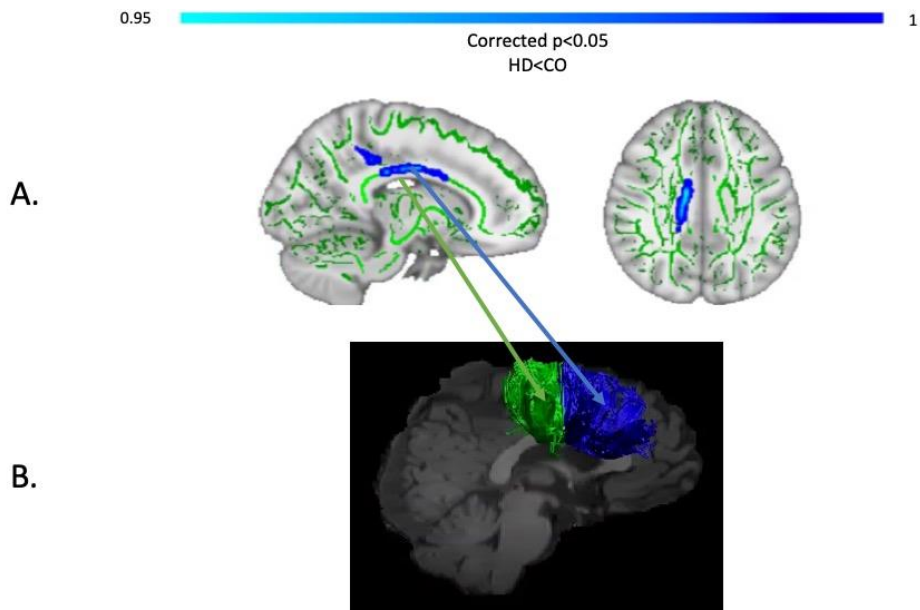


623

624 **Figure 5.**

625

626



627

628 **Figure 6.**

629

630

631

632

633

634

635 **Funding & Acknowledgements**

636 The present research was funded by a Wellcome Trust Institutional Strategic Support

637 Fund Award (ref: 506408) to CMB, AR, and DKJ and a Wellcome Trust PhD

638 studentship to CC (ref: 204005/Z/16/Z); DKJ is supported by a New Investigator Award

639 from the Wellcome Trust (ref: 096646/Z/11/Z). We would like to thank Candace

640 Ferman and Louise Gethin for collating the patients' clinical details and Jilu Mole for

641 assistance with data analysis. This manuscript has been released as a pre-print at

642 bioRxiv: <https://biorxiv.org/cgi/content/short/2019.12.24.887406v1>

643

644

645 **References**

- 646 [1] Weaver KE, Richards TL, Liang O, Laurino MY, Samii A, Aylward EH. Longitudinal
647 diffusion tensor imaging in Huntington's Disease. *Exp Neurol* 2009;216:525–9.
648 <https://doi.org/10.1016/j.expneurol.2008.12.026>.
- 649 [2] Bardile CF, Garcia-Miralles M, Caron N, Langley S, Teo RTY, Petretto E, et al. A43
650 Intrinsic mutant HTT-mediated defects in oligodendroglia cells contribute to myelin
651 deficits and behavioural abnormalities in huntington disease. *J Neurol Neurosurg
652 Psychiatry* 2018;89:A15–6. <https://doi.org/10.1136/jnnp-2018-EHDN.41>.
- 653 [3] Bartzokis G, Lu PH, Tishler TA, Fong SM, Oluwadara B, Finn JP, et al. Myelin
654 breakdown and iron changes in Huntington's disease: pathogenesis and treatment
655 implications. *Neurochem Res* 2007;32:1655–64. [https://doi.org/10.1007/s11064-007-](https://doi.org/10.1007/s11064-007-9352-7)
656 [9352-7](https://doi.org/10.1007/s11064-007-9352-7).
- 657 [4] Beglinger LJ, Langbehn DR, Duff K, Stierman L, Black DW, Nehl C, et al. Probability
658 of obsessive and compulsive symptoms in Huntington's disease. *Biol Psychiatry*
659 2007;61:415–8. <https://doi.org/10.1016/j.biopsych.2006.04.034>.
- 660 [5] Ciarmiello A, Cannella M, Lastoria S, Simonelli M, Frati L, Rubinsztein DC, et al. Brain
661 white-matter volume loss and glucose hypometabolism precede the clinical symptoms
662 of Huntington's disease. *J Nucl Med Off Publ Soc Nucl Med* 2006;47:215–22.
- 663 [6] Gregory S, Crawford H, Seunarine K, Leavitt B, Durr A, Roos RAC, et al. Natural
664 biological variation of white matter microstructure is accentuated in Huntington's
665 disease. *Hum Brain Mapp* 2018;39:3516–27. <https://doi.org/10.1002/hbm.24191>.
- 666 [7] Paulsen JS, Langbehn DR, Stout JC, Aylward E, Ross CA, Nance M, et al. Detection of
667 Huntington's disease decades before diagnosis: the Predict-HD study. *J Neurol
668 Neurosurg Psychiatry* 2008;79:874–80. <https://doi.org/10.1136/jnnp.2007.128728>.

- 669 [8] Rosas HD, Wilkens P, Salat DH, Mercaldo ND, Vangel M, Yendiki AY, et al. Complex
670 spatial and temporally defined myelin and axonal degeneration in Huntington disease.
671 *NeuroImage Clin* 2018;20:236–42. <https://doi.org/10.1016/j.nicl.2018.01.029>.
- 672 [9] Wang N, Yang XW. Huntington Disease’s Glial Progenitor Cells Hit the Pause Button in
673 the Mouse Brain. *Cell Stem Cell* 2019;24:3–4.
674 <https://doi.org/10.1016/j.stem.2018.12.004>.
- 675 [10] Gómez-Tortosa E, MacDonald ME, Friend JC, Taylor SA, Weiler LJ, Cupples LA, et al.
676 Quantitative neuropathological changes in presymptomatic Huntington’s disease. *Ann*
677 *Neurol* 2001;49:29–34.
- 678 [11] Huang B, Wei W, Wang G, Gaertig MA, Feng Y, Wang W, et al. Mutant huntingtin
679 downregulates myelin regulatory factor-mediated myelin gene expression and affects
680 mature oligodendrocytes. *Neuron* 2015;85:1212–26.
681 <https://doi.org/10.1016/j.neuron.2015.02.026>.
- 682 [12] Jin J, Peng Q, Hou Z, Jiang M, Wang X, Langseth AJ, et al. Early white matter
683 abnormalities, progressive brain pathology and motor deficits in a novel knock-in mouse
684 model of Huntington’s disease. *Hum Mol Genet* 2015;24:2508–27.
685 <https://doi.org/10.1093/hmg/ddv016>.
- 686 [13] Myers RH, Vonsattel JP, Paskevich PA, Kiely DK, Stevens TJ, Cupples LA, et al.
687 Decreased Neuronal and Increased Oligodendroglial Densities in Huntington’s Disease
688 Caudate Nucleus. *J Neuropathol Exp Neurol* 1991;50:729–42.
689 <https://doi.org/10.1097/00005072-199111000-00005>.
- 690 [14] Simmons DA, Casale M, Alcon B, Pham N, Narayan N, Lynch G. Ferritin accumulation
691 in dystrophic microglia is an early event in the development of Huntington’s disease.
692 *Glia* n.d.;55:1074–84. <https://doi.org/10.1002/glia.20526>.

- 693 [15] Teo RTY, Hong X, Yu-Taeger L, Huang Y, Tan LJ, Xie Y, et al. Structural and molecular
694 myelination deficits occur prior to neuronal loss in the YAC128 and BACHD models of
695 Huntington disease. *Hum Mol Genet* 2016;25:2621–32.
696 <https://doi.org/10.1093/hmg/ddw122>.
- 697 [16] Martenson RE. *Myelin*. CRC Press; 1992.
- 698 [17] Han I, You Y, Kordower JH, Brady ST, Morfini GA. Differential vulnerability of neurons
699 in Huntington’s disease: the role of cell type-specific features. *J Neurochem*
700 2010;113:1073–91. <https://doi.org/10.1111/j.1471-4159.2010.06672.x>.
- 701 [18] Barker R, Mason SL. The hunt for better treatments for Huntington’s disease. *Lancet*
702 *Neurol* 2019;18:131–3. [https://doi.org/10.1016/S1474-4422\(18\)30448-4](https://doi.org/10.1016/S1474-4422(18)30448-4).
- 703 [19] Shannon KM. Recent Advances in the Treatment of Huntington’s Disease: Targeting
704 DNA and RNA. *CNS Drugs* 2020;34:219–28. [https://doi.org/10.1007/s40263-019-](https://doi.org/10.1007/s40263-019-00695-3)
705 [00695-3](https://doi.org/10.1007/s40263-019-00695-3).
- 706 [20] Wood NI, Glynn D, Morton AJ. “Brain training” improves cognitive performance and
707 survival in a transgenic mouse model of Huntington’s disease. *Neurobiol Dis*
708 2011;42:427–37. <https://doi.org/10.1016/j.nbd.2011.02.005>.
- 709 [21] Yhnell E, Lelos MJ, Dunnett SB, Brooks SP. Cognitive training modifies disease
710 symptoms in a mouse model of Huntington’s disease. *Exp Neurol* 2016;282:19–26.
711 <https://doi.org/10.1016/j.expneurol.2016.05.008>.
- 712 [22] Yhnell E, Furby H, Breen RS, Brookes-Howell LC, Drew CJG, Playle R, et al. Exploring
713 computerised cognitive training as a therapeutic intervention for people with
714 Huntington’s disease (CogTrainHD): protocol for a randomised feasibility study. *Pilot*
715 *Feasibility Stud* 2018;4:45. <https://doi.org/10.1186/s40814-018-0237-0>.

- 716 [23] Caeyenberghs K, Metzler-Baddeley C, Foley S, Jones DK. Dynamics of the Human
717 Structural Connectome Underlying Working Memory Training. *J Neurosci Off J Soc*
718 *Neurosci* 2016;36:4056–66. <https://doi.org/10.1523/JNEUROSCI.1973-15.2016>.
- 719 [24] Taubert M, Lohmann G, Margulies DS, Villringer A, Ragert P. Long-term effects of
720 motor training on resting-state networks and underlying brain structure. *NeuroImage*
721 2011;57:1492–8. <https://doi.org/10.1016/j.neuroimage.2011.05.078>.
- 722 [25] Metzler-Baddeley C, Cantera J, Coulthard E, Rosser A, Jones DK, Baddeley RJ.
723 Improved Executive Function and Callosal White Matter Microstructure after Rhythm
724 Exercise in Huntington’s Disease. *J Huntingt Dis* 2014;3:273–83.
725 <https://doi.org/10.3233/JHD-140113>.
- 726 [26] Drijkoningen D, Caeyenberghs K, Leunissen I, Vander Linden C, Leemans A, Sunaert S,
727 et al. Training-induced improvements in postural control are accompanied by alterations
728 in cerebellar white matter in brain injured patients. *NeuroImage Clin* 2014;7:240–51.
729 <https://doi.org/10.1016/j.nicl.2014.12.006>.
- 730 [27] Scholz J, Klein MC, Behrens TEJ, Johansen-Berg H. Training induces changes in white
731 matter architecture. *Nat Neurosci* 2009;12:1370–1. <https://doi.org/10.1038/nn.2412>.
- 732 [28] Hu Y, Geng F, Tao L, Hu N, Du F, Fu K, et al. Enhanced white matter tracts integrity in
733 children with abacus training. *Hum Brain Mapp* 2011;32:10–21.
734 <https://doi.org/10.1002/hbm.20996>.
- 735 [29] Bengtsson SL, Nagy Z, Skare S, Forsman L, Forssberg H, Ullén F. Extensive piano
736 practicing has regionally specific effects on white matter development. *Nat Neurosci*
737 2005;8:1148–50. <https://doi.org/10.1038/nn1516>.
- 738 [30] Han Y, Yang H, Lv Y-T, Zhu C-Z, He Y, Tang H-H, et al. Gray matter density and white
739 matter integrity in pianists’ brain: A combined structural and diffusion tensor MRI study.
740 *Neurosci Lett* 2009;459:3–6. <https://doi.org/10.1016/j.neulet.2008.07.056>.

- 741 [31] Takeuchi H, Sekiguchi A, Taki Y, Yokoyama S, Yomogida Y, Komuro N, et al. Training
742 of working memory impacts structural connectivity. *J Neurosci Off J Soc Neurosci*
743 2010;30:3297–303. <https://doi.org/10.1523/JNEUROSCI.4611-09.2010>.
- 744 [32] Mackey A, Whitaker K, Bunge S. Experience-dependent plasticity in white matter
745 microstructure: reasoning training alters structural connectivity. *Front Neuroanat*
746 2012;6:32. <https://doi.org/10.3389/fnana.2012.00032>.
- 747 [33] Tang Y-Y, Lu Q, Fan M, Yang Y, Posner MI. Mechanisms of white matter changes
748 induced by meditation. *Proc Natl Acad Sci* 2012;109:10570–4.
749 <https://doi.org/10.1073/pnas.1207817109>.
- 750 [34] Caeyenberghs K, Clemente A, Imms P, Egan G, Hocking DR, Leemans A, et al. Evidence
751 for Training-Dependent Structural Neuroplasticity in Brain-Injured Patients: A Critical
752 Review. *Neurorehabil Neural Repair* 2018;32:99–114.
753 <https://doi.org/10.1177/1545968317753076>.
- 754 [35] Gibson EM, Purger D, Mount CW, Goldstein AK, Lin GL, Wood LS, et al. Neuronal
755 Activity Promotes Oligodendrogenesis and Adaptive Myelination in the Mammalian
756 Brain. *Science* 2014;344:1252304. <https://doi.org/10.1126/science.1252304>.
- 757 [36] Mensch S, Baraban M, Almeida R, Czopka T, Ausborn J, El Manira A, et al. Synaptic
758 vesicle release regulates myelin sheath number of individual oligodendrocytes in vivo.
759 *Nat Neurosci* 2015;18:628–30. <https://doi.org/10.1038/nn.3991>.
- 760 [37] Sampaio-Baptista C, Khrapitchev AA, Foxley S, Schlagheck T, Scholz J, Jbabdi S, et al.
761 Motor Skill Learning Induces Changes in White Matter Microstructure and Myelination.
762 *J Neurosci* 2013;33:19499–503. <https://doi.org/10.1523/JNEUROSCI.3048-13.2013>.
- 763 [38] Lakhani B, Borich MR, Jackson JN, Wadden KP, Peters S, Villamayor A, et al. Motor
764 Skill Acquisition Promotes Human Brain Myelin Plasticity. *Neural Plast*
765 2016;2016:7526135. <https://doi.org/10.1155/2016/7526135>.

- 766 [39] Costa RM, Cohen D, Nicolelis MAL. Differential corticostriatal plasticity during fast and
767 slow motor skill learning in mice. *Curr Biol CB* 2004;14:1124–34.
768 <https://doi.org/10.1016/j.cub.2004.06.053>.
- 769 [40] Shmuelof L, Krakauer JW. Are we ready for a natural history of motor learning? *Neuron*
770 2011;72:469–76. <https://doi.org/10.1016/j.neuron.2011.10.017>.
- 771 [41] Steele CJ, Bailey JA, Zatorre RJ, Penhune VB. Early musical training and white-matter
772 plasticity in the corpus callosum: evidence for a sensitive period. *J Neurosci Off J Soc*
773 *Neurosci* 2013;33:1282–90. <https://doi.org/10.1523/JNEUROSCI.3578-12.2013>.
- 774 [42] Yin HH, Mulcare SP, Hilário MRF, Clouse E, Holloway T, Davis MI, et al. Dynamic
775 reorganization of striatal circuits during the acquisition and consolidation of a skill. *Nat*
776 *Neurosci* 2009;12:333–41. <https://doi.org/10.1038/nn.2261>.
- 777 [43] Sagi Y, Tavor I, Hofstetter S, Tzur-Moryosef S, Blumenfeld-Katzir T, Assaf Y. Learning
778 in the Fast Lane: New Insights into Neuroplasticity. *Neuron* 2012;73:1195–203.
779 <https://doi.org/10.1016/j.neuron.2012.01.025>.
- 780 [44] Xiao L, Ohayon D, McKenzie IA, Sinclair-Wilson A, Wright JL, Fudge AD, et al. Rapid
781 production of new oligodendrocytes is required in the earliest stages of motor skill
782 learning. *Nat Neurosci* 2016;19:1210–7. <https://doi.org/10.1038/nn.4351>.
- 783 [45] Papoutsis M, Labuschagne I, Tabrizi SJ, Stout JC. The cognitive burden in Huntington’s
784 disease: Pathology, phenotype, and mechanisms of compensation. *Mov Disord*
785 2014;29:673–83. <https://doi.org/10.1002/mds.25864>.
- 786 [46] Nakamura T, Nagata M, Yagi T, Graybiel AM, Yamamori T, Kitsukawa T. Learning new
787 sequential stepping patterns requires striatal plasticity during the earliest phase of
788 acquisition. *Eur J Neurosci* 2017;45:901–11. <https://doi.org/10.1111/ejn.13537>.

- 789 [47] Lanciego JL, Luquin N, Obeso JA. Functional neuroanatomy of the basal ganglia. *Cold*
790 *Spring Harb Perspect Med* 2012;2:a009621–a009621.
791 <https://doi.org/10.1101/cshperspect.a009621>.
- 792 [48] Guitart NA, Connelly DM, Nagamatsu LS, Orange JB, Muir-Hunter SW. The effects of
793 physical exercise on executive function in community-dwelling older adults living with
794 Alzheimer’s-type dementia: A systematic review. *Ageing Res Rev* 2018;47:159–67.
795 <https://doi.org/10.1016/j.arr.2018.07.009>.
- 796 [49] Duchesne C, Lungu O, Nadeau A, Robillard ME, Boré A, Bobeuf F, et al. Enhancing both
797 motor and cognitive functioning in Parkinson’s disease: Aerobic exercise as a
798 rehabilitative intervention. *Brain Cogn* 2015;99:68–77.
799 <https://doi.org/10.1016/j.bandc.2015.07.005>.
- 800 [50] Giacosa C, Karpati FJ, Foster NEV, Penhune VB, Hyde KL. Dance and music training
801 have different effects on white matter diffusivity in sensorimotor pathways. *NeuroImage*
802 2016;135:273–86. <https://doi.org/10.1016/j.neuroimage.2016.04.048>.
- 803 [51] Pierpaoli C, Basser PJ. Toward a quantitative assessment of diffusion anisotropy. *Magn*
804 *Reson Med* 1996;36:893–906.
- 805 [52] De Santis S, Drakesmith M, Bells S, Assaf Y, Jones DK. Why diffusion tensor MRI does
806 well only some of the time: Variance and covariance of white matter tissue
807 microstructure attributes in the living human brain. *Neuroimage* 2014;89:35–44.
808 <https://doi.org/10.1016/j.neuroimage.2013.12.003>.
- 809 [53] Wheeler-Kingshott CAM, Cercignani M. About “axial” and “radial” diffusivities. *Magn*
810 *Reson Med* 2009;61:1255–60. <https://doi.org/10.1002/mrm.21965>.
- 811 [54] Sled JG. Modelling and interpretation of magnetization transfer imaging in the brain.
812 *NeuroImage* 2018;182:128–35. <https://doi.org/10.1016/j.neuroimage.2017.11.065>.

- 813 [55] Assaf Y, Basser PJ. Composite hindered and restricted model of diffusion (CHARMED)
814 MR imaging of the human brain. *NeuroImage* 2005;27:48–58.
815 <https://doi.org/10.1016/j.neuroimage.2005.03.042>.
- 816 [56] Lövdén M, Bodammer NC, Kühn S, Kaufmann J, Schütze H, Tempelmann C, et al.
817 Experience-dependent plasticity of white-matter microstructure extends into old age.
818 *Neuropsychologia* 2010;48:3878–83.
819 <https://doi.org/10.1016/j.neuropsychologia.2010.08.026>.
- 820 [57] Zatorre RJ, Fields RD, Johansen-Berg H. Plasticity in gray and white: neuroimaging
821 changes in brain structure during learning. *Nat Neurosci* 2012;15:528–36.
822 <https://doi.org/10.1038/nn.3045>.
- 823 [58] Serres S, Anthony DC, Jiang Y, Campbell SJ, Broom KA, Khrapitchev A, et al.
824 Comparison of MRI signatures in pattern I and II multiple sclerosis models. *NMR*
825 *Biomed* 2009;22:1014–24. <https://doi.org/10.1002/nbm.1404>.
- 826 [59] Ou X, Sun S-W, Liang H-F, Song S-K, Gochberg DF. The MT pool size ratio and the
827 DTI radial diffusivity may reflect the myelination in shiverer and control mice. *NMR*
828 *Biomed* 2009;22:480–7. <https://doi.org/10.1002/nbm.1358>.
- 829 [60] Levesque IR, Giacomini PS, Narayanan S, Ribeiro LT, Sled JG, Arnold DL, et al.
830 Quantitative magnetization transfer and myelin water imaging of the evolution of acute
831 multiple sclerosis lesions. *Magn Reson Med* 2010;63:633–40.
832 <https://doi.org/10.1002/mrm.22244>.
- 833 [61] Schmierer K, Tozer DJ, Scaravilli F, Altmann DR, Barker GJ, Tofts PS, et al. Quantitative
834 Magnetization Transfer Imaging in Postmortem Multiple Sclerosis Brain. *J Magn Reson*
835 *Imaging JMRI* 2007;26:41–51. <https://doi.org/10.1002/jmri.20984>.

- 836 [62] Barazany D, Basser PJ, Assaf Y. In vivo measurement of axon diameter distribution in
837 the corpus callosum of rat brain. *Brain* 2009;132:1210–20.
838 <https://doi.org/10.1093/brain/awp042>.
- 839 [63] Poudel GR, Stout JC, Domínguez D JF, Salmon L, Churchyard A, Chua P, et al. White
840 matter connectivity reflects clinical and cognitive status in Huntington’s disease.
841 *Neurobiol Dis* 2014;65:180–7. <https://doi.org/10.1016/j.nbd.2014.01.013>.
- 842 [64] Hofer S, Frahm J. Topography of the human corpus callosum revisited--comprehensive
843 fiber tractography using diffusion tensor magnetic resonance imaging. *NeuroImage*
844 2006;32:989–94. <https://doi.org/10.1016/j.neuroimage.2006.05.044>.
- 845 [65] Vonsattel JPG, Difiglia M. Huntington Disease. *J Neuropathol Exp Neurol* 1998;57:369–
846 84. <https://doi.org/10.1097/00005072-199805000-00001>.
- 847 [66] Diana Rosas H, Lee SY, Bender A, Zaleta AK, Vange M, Yu P, et al. Altered White
848 Matter Microstructure in the Corpus Callosum in Huntington’s Disease: implications for
849 cortical “disconnection.” *NeuroImage* 2010;49:2995–3004.
850 <https://doi.org/10.1016/j.neuroimage.2009.10.015>.
- 851 [67] Phillips O, Sanchez-Castaneda C, Elifani F, Maglione V, Pardo AD, Caltagirone C, et al.
852 Tractography of the Corpus Callosum in Huntington’s Disease. *PLOS ONE*
853 2013;8:e73280. <https://doi.org/10.1371/journal.pone.0073280>.
- 854 [68] Dumas EM, van den Bogaard SJA, Ruber ME, Reilman RR, Stout JC, Craufurd D, et al.
855 Early changes in white matter pathways of the sensorimotor cortex in premanifest
856 Huntington’s disease. *Hum Brain Mapp* 2012;33:203–12.
857 <https://doi.org/10.1002/hbm.21205>.
- 858 [69] Bourbon-Teles J, Bells S, Jones DK, Coulthard E, Rosser A, Metzler-Baddeley C. Myelin
859 Breakdown in Human Huntington’s Disease: Multi-Modal Evidence from Diffusion

860 MRI and Quantitative Magnetization Transfer. *Non-Invasive MRI Window Brain*
861 *Inflamm* 2019;403:79–92. <https://doi.org/10.1016/j.neuroscience.2017.05.042>.

862 [70] Smith SM, Jenkinson M, Johansen-Berg H, Rueckert D, Nichols TE, Mackay CE, et al.
863 Tract-based spatial statistics: Voxelwise analysis of multi-subject diffusion data.
864 *NeuroImage* 2006;31:1487–505. <https://doi.org/10.1016/j.neuroimage.2006.02.024>.

865 [71] Nasreddine ZS, Phillips NA, Bédirian V, Charbonneau S, Whitehead V, Collin I, et al.
866 The Montreal Cognitive Assessment, MoCA: A Brief Screening Tool For Mild
867 Cognitive Impairment. *J Am Geriatr Soc* 2005;53:695–9. [https://doi.org/10.1111/j.1532-](https://doi.org/10.1111/j.1532-5415.2005.53221.x)
868 [5415.2005.53221.x](https://doi.org/10.1111/j.1532-5415.2005.53221.x).

869 [72] Nelson H. National Adult Reading Test (NART) test manual (Part 1 n.d.

870 [73] Baddeley A. Exploring the central executive. *Q J Exp Psychol A* 1996;49A:5–28.
871 <https://doi.org/10.1080/027249896392784>.

872 [74] Baldo JV, Shimamura AP, Delis DC, Kramer J, Kaplan E. Verbal and design fluency in
873 patients with frontal lobe lesions. *J Int Neuropsychol Soc* 2001;7:586–96.
874 <https://doi.org/10.1017/S1355617701755063>.

875 [75] Jones DK, Horsfield MA, Simmons A. Optimal strategies for measuring diffusion in
876 anisotropic systems by magnetic resonance imaging. *Magn Reson Med* 1999;42:515–
877 25.

878 [76] Cercignani M, Alexander DC. Optimal acquisition schemes for in vivo quantitative
879 magnetization transfer MRI. *Magn Reson Med* 2006;56:803–10.
880 <https://doi.org/10.1002/mrm.21003>.

881 [77] Irfanoglu MO, Walker L, Sarlls J, Marengo S, Pierpaoli C. Effects of image distortions
882 originating from susceptibility variations and concomitant fields on diffusion MRI
883 tractography results. *NeuroImage* 2012;61:275–88.
884 <https://doi.org/10.1016/j.neuroimage.2012.02.054>.

- 885 [78] Leemans A, Jones DK. The B-matrix must be rotated when correcting for subject motion
886 in DTI data. *Magn Reson Med* 2009;61:1336–49. <https://doi.org/10.1002/mrm.21890>.
- 887 [79] Leemans A, Jeurissen B, Sijbers J, Jones D. ExploreDTI: a graphical toolbox for
888 processing, analyzing, and visualizing diffusion MR data. *Proc Intl Soc Mag Reson Med*,
889 vol. 17, 2009.
- 890 [80] Pasternak O, Sochen N, Gur Y, Intrator N, Assaf Y. Free water elimination and mapping
891 from diffusion MRI. *Magn Reson Med* 2009;62:717–30.
892 <https://doi.org/10.1002/mrm.22055>.
- 893 [81] Ben-Amitay S, Jones DK, Assaf Y. Motion correction and registration of high b-value
894 diffusion weighted images. *Magn Reson Med* 2012;67:1694–702.
895 <https://doi.org/10.1002/mrm.23186>.
- 896 [82] Klein S, Staring M, Murphy K, Viergever MA, Pluim JPW. elastix: a toolbox for
897 intensity-based medical image registration. *IEEE Trans Med Imaging* 2010;29:196–205.
898 <https://doi.org/10.1109/TMI.2009.2035616>.
- 899 [83] Henkelman RM, Huang X, Xiang QS, Stanisz GJ, Swanson SD, Bronskill MJ.
900 Quantitative interpretation of magnetization transfer. *Magn Reson Med* 1993;29:759–
901 66.
- 902 [84] Ramani A, Dalton C, Miller DH, Tofts PS, Barker GJ. Precise estimate of fundamental
903 in-vivo MT parameters in human brain in clinically feasible times. *Magn Reson Imaging*
904 2002;20:721–31. [https://doi.org/10.1016/S0730-725X\(02\)00598-2](https://doi.org/10.1016/S0730-725X(02)00598-2).
- 905 [85] Dell’acqua F, Scifo P, Rizzo G, Catani M, Simmons A, Scotti G, et al. A modified damped
906 Richardson-Lucy algorithm to reduce isotropic background effects in spherical
907 deconvolution. *NeuroImage* 2010;49:1446–58.
908 <https://doi.org/10.1016/j.neuroimage.2009.09.033>.

- 909 [86] Jeurissen B, Leemans A, Jones DK, Tournier J-D, Sijbers J. Probabilistic fiber tracking
910 using the residual bootstrap with constrained spherical deconvolution. *Hum Brain Mapp*
911 2011;32:461–79. <https://doi.org/10.1002/hbm.21032>.
- 912 [87] Catani M, Howard RJ, Pajevic S, Jones DK. Virtual in vivo interactive dissection of white
913 matter fasciculi in the human brain. *NeuroImage* 2002;17:77–94.
914 <https://doi.org/10.1006/nimg.2002.1136>.
- 915 [88] Leh SE, Ptito A, Chakravarty MM, Strafella AP. Fronto-striatal connections in the human
916 brain: a probabilistic diffusion tractography study. *Neurosci Lett* 2007;419:113–8.
917 <https://doi.org/10.1016/j.neulet.2007.04.049>.
- 918 [89] Mair P, Wilcox R. Robust statistical methods in R using the WRS2 package. *Behav Res*
919 *Methods* 2020;52:464–88. <https://doi.org/10.3758/s13428-019-01246-w>.
- 920 [90] Wilcox RR. Introduction to robust estimation and hypothesis testing. Academic press;
921 2011.
- 922 [91] Testa R, Bennett P, Ponsford J. Factor analysis of nineteen executive function tests in a
923 healthy adult population. *Arch Clin Neuropsychol Off J Natl Acad Neuropsychol*
924 2012;27:213–24. <https://doi.org/10.1093/arclin/acr112>.
- 925 [92] Preacher KJ, MacCallum RC. Exploratory Factor Analysis in Behavior Genetics
926 Research: Factor Recovery with Small Sample Sizes. *Behav Genet* 2002;32:153–61.
927 <https://doi.org/10.1023/A:1015210025234>.
- 928 [93] Winter* JCF de, Dodou* D, Wieringa PA. Exploratory Factor Analysis With Small
929 Sample Sizes. *Multivar Behav Res* 2009;44:147–81.
930 <https://doi.org/10.1080/00273170902794206>.
- 931 [94] Cattell RB. The Scree Test For The Number Of Factors. *Multivar Behav Res* 1966;1:245–
932 76. https://doi.org/10.1207/s15327906mbr0102_10.
- 933 [95] Cohen J. Statistical power analysis for the behavioral sciences. Academic press; 2013.

- 934 [96] Benjamini Y, Hochberg Y. Controlling the False Discovery Rate: A Practical and
935 Powerful Approach to Multiple Testing. *J R Stat Soc Ser B Methodol* 1995;57:289–300.
- 936 [97] Penke L, Maniega SM, Murray C, Gow AJ, Hernández MCV, Clayden JD, et al. A
937 General Factor of Brain White Matter Integrity Predicts Information Processing Speed
938 in Healthy Older People. *J Neurosci* 2010;30:7569–74.
939 <https://doi.org/10.1523/JNEUROSCI.1553-10.2010>.
- 940 [98] Wahl M, Li Y-O, Ng J, Lahue SC, Cooper SR, Sherr EH, et al. Microstructural
941 correlations of white matter tracts in the human brain. *NeuroImage* 2010;51:531–41.
942 <https://doi.org/10.1016/j.neuroimage.2010.02.072>.
- 943 [99] Westfall J, Yarkoni T. Statistically Controlling for Confounding Constructs Is Harder than
944 You Think. *PLOS ONE* 2016;11:e0152719.
945 <https://doi.org/10.1371/journal.pone.0152719>.
- 946 [100] Henkelman RM, Stanisz GJ, Graham SJ. Magnetization transfer in MRI: a review. *NMR*
947 *Biomed n.d.*;14:57–64. <https://doi.org/10.1002/nbm.683>.
- 948 [101] Rocha NP, Ribeiro FM, Furr-Stimming E, Teixeira AL. Neuroimmunology of
949 Huntington’s disease: revisiting evidence from human studies. *Mediators Inflamm*
950 2016;2016.
- 951 [102] Vinther-Jensen T, Simonsen AH, Budtz-Jørgensen E, Hjermand LE, Nielsen JE.
952 Ubiquitin: a potential cerebrospinal fluid progression marker in Huntington’s disease.
953 *Eur J Neurol n.d.*;22:1378–84. <https://doi.org/10.1111/ene.12750>.
- 954 [103] Wang Y, van Gelderen P, de Zwart JA, Duyn JH. B0-field dependence of MRI T1
955 relaxation in human brain. *NeuroImage* 2020;213:116700.
956 <https://doi.org/10.1016/j.neuroimage.2020.116700>.

- 957 [104] Chomiak T, Hu B. What Is the Optimal Value of the g-Ratio for Myelinated Fibers in
958 the Rat CNS? A Theoretical Approach. PLOS ONE 2009;4:e7754.
959 <https://doi.org/10.1371/journal.pone.0007754>.
- 960 [105] Kaller MS, Lazari A, Blanco-Duque C, Sampaio-Baptista C, Johansen-Berg H. Myelin
961 plasticity and behaviour—connecting the dots. *Curr Opin Neurobiol* 2017;47:86–92.
962 <https://doi.org/10.1016/j.conb.2017.09.014>.
- 963 [106] Rushton WAH. A theory of the effects of fibre size in medullated nerve. *J Physiol*
964 1951;115:101–22.
- 965 [107] Valkanova V, Eguia Rodriguez R, Ebmeier KP. Mind over matter--what do we know
966 about neuroplasticity in adults? *Int Psychogeriatr* 2014;26:891–909.
967 <https://doi.org/10.1017/S1041610213002482>.
- 968 [108] Thomas C, Baker CI. Teaching an adult brain new tricks: A critical review of evidence
969 for training-dependent structural plasticity in humans. *NeuroImage* 2013;73:225–36.
970 <https://doi.org/10.1016/j.neuroimage.2012.03.069>.
- 971 [109] Trener MR, Crosson B, DeBoe J, Leber WR. Stroop neuropsychological screening
972 test. *Odessa FL Psychol Assess Resour* 1989.
- 973 [110] Delis DC, Kramer JH, Kaplan E, Holdnack J. Reliability and validity of the Delis-Kaplan
974 Executive Function System: an update. *J Int Neuropsychol Soc JINS* 2004;10:301–3.
975 <https://doi.org/10.1017/S1355617704102191>.
- 976
- 977

	Age	Length of CAG repeats	TMS	FAS
Mean	48.5	43.6	18.7	22.6
(Range)	(22-68)	(40-51)	(0-69)	(17-25)
SD	15.6	3.5	24.7	3.3

978

979 **Table 1.** Demographics and background clinical information of the patients' cohort.

980 Based on TMS and FAS, most of the patients were at early disease stages, however

981 two of them were more advanced. Abbreviations: CAG = cytosine-adenine-guanine;

982 TMS = Total Motor Score out of 124 (the higher the scores the more impaired the

983 performance); FAS = Functional Assessment Score out of 25 (the higher the scores

984 the better the performance); SD = Standard Deviation.

985

986

Mean (SD, range)	Patients (n = 8)	Controls (n = 9)	Mann-Whitney U (p-value)
Age	48.5 (15.62, 22-68)	52.6 (14.56, 22-68)	U = 31 (p = 0.673)
NART-IQ	106.3 (13.13, 94-123)	121.22 (4.32, 117-128)	U = 8 (p = 0.006)
MoCa	23 (5.6, 14-29)	27.67 (1, 26-29)	U = 14 (p = 0.036)

987

988 **Table 2.** Demographics and general cognitive profile of patients and controls. Both

989 groups were matched for age, sex and years of education but the patient group had a

990 lower NART-IQ and performed less well than the control group in the MoCA.
 991 Abbreviations: NART-IQ = verbal IQ estimate based on the National Adult Reading
 992 Test; MoCA = Montreal Cognitive Assessment score out of 30.
 993
 994

Task	Outcome variables	Description
Simultaneous box crossing and digit sequences repetition [73]	Correct digits recalled under single task condition; correct digits recalled under dual task conditions; boxes identified under dual task condition.	Correct number of recalled digits in a standard digit span test; correct number of recalled digits in the dual condition; number of boxes identified in the dual condition
Stroop test [109]	Stroop interference score	Calculated by subtracting the number of errors from the total number of items presented in the test
Trials test [73]	Trail test switching	Performance accuracy: reflects the ability of moving flexibly from one set of rules to another in response to changing task requirements

Verbal and category fluency test [110]

Verbal and category fluency

Number of generated words starting with the following letters: “F”, “A”, “S” and “M”, “C”, “R”; number of generated words belonging to the following categories: “animals” and “boys’ names” and “supermarket items” and “girls’ names”

995 **Table 3.** Cognitive outcome variables assessed in this study. Tests were carried out
 996 before and after the training, and a percentage change score was computed for each
 997 variable.

998
 999

1000

	T ₁ -w	DTI	CHARME D	T1 map	MT-w	B0 map
Pulse sequence	FSPGR	SE\EPI	SE\EPI	SPGR (3D)	FSPGR (3D)	SPGR (3D)
Matrix size	256x256	96x96	96x96	96x96x60	96x96x60	128x128
FoV (mm)	230	230	230	240	240	220
Slices	172	60	60	-	-	-

Slice thickness (mm)	1	2.4	2.4	-	-	-
TE,TR (ms)	7.8, 2.9	87, 16000	126, 17000	6.85, 1.2	2.18,25.82	TE: 9 & 7 TR: 20
Off-resonance pulses (Hz/°)	-	-	-	-	100[38]0/332, - 1000/333, 12062/628, 47185/628, 56363/332, 2751/628, 1000/628, 1000/628, 2768/628, 2791/628, 2887/628	
Flip angles (°)	20	90	90	15,7,3	5	90

1001 **Table 4.** Scan parameters. All sequences were acquired at 3T. For each of the
1002 sequences, the main acquisition parameters are provided. T_1 -w: T_1 -weighted; MT-w:
1003 MT-weighted; FSPGR: fast spoiled gradient echo; SE: spin-echo; EPI: echo-planar
1004 imaging; SPGR: spoiled gradient recalled-echo; FoV: field of view; TE: echo time; TR:
1005 repetition time.
1006
1007

% Change	Executive	Working memory capacity	Fluency
Total box (dual)	0.864	0.022	0.419
Stroop interference score	0.811	-0.270	-0.267
Trail test switching	0.731	-0.470	0.162
Correct digits under single task condition	0.201	0.904	0.129
Correct digits under dual task condition	-0.193	0.855	-0.018
Category fluency	-0.070	-0.138	0.817
Verbal fluency	-0.026	-0.232	-0.799

1009 **Table 5.** Rotated Component Loadings on Change in the Cognitive Benchmark Tests.

1010 Significant loadings (>0.5) are highlighted in bold.

1011

1012

FA	t	p	FDR corrected p
CCI	1.220	0.909	0.91
CCII	2.650	0.91	0.91

CCIII	0.320	0.48	0.91
Left SMA-Putamen	5.160	0.77	0.91
Right SMA-Putamen	-9.54	0.02	0.11

RD

CCI	-0.48	0.35	0.45
CCII	-1.29	0.22	0.45
CCIII	-1.04	0.30	0.45
Left SMA-Putamen	-3.68	0.08	0.39
Right SMA-Putamen	4.010	0.80	0.80

Fr

CCI	0.033	0.81	0.82
CCII	-0.001	0.49	0.82
CCIII	0.03	0.82	0.82
Left SMA-Putamen	0.01	0.58	0.82
Right SMA-Putamen	-0.052	0.1996	0.817

MPF

CCI	-12.06	0.08	0.10
CCII	-20.72	0.03	0.05

CCIII	-25.87	0.02	0.05
Left SMA-Putamen	-4.34	0.38	0.38
Right SMA-Putamen	-25.48	0.02	0.05

1013 **Table 6.** Summary statistics for the permutation analysis of training effects on FA, RD,
1014 Fr and MPF, across the investigated tracts.

1015
1016
1017
1018

1019 **Figure 1. (1) pathway regions of interest.** Sagittal views of the reconstructed WM
1020 pathways displayed on a T_1 -weighted image for one control participant. (A) CCI, CCII,
1021 and CCIII (Hofer and Frahm, 2006): CCI is the most anterior portion of the CC and
1022 maintains prefrontal connections between both hemispheres; CCII is the portion that
1023 maintains connections between premotor and supplementary motor areas of both
1024 hemispheres. CCIII maintains connections between primary motor cortices of both
1025 hemispheres. (B) SMA-putamen pathway: this pathway has efferent and afferent
1026 projections to the primary motor cortex and is involved in movement execution.

1027

1028 **Figure 2. Sagittal views of the tractography protocols.** (A) CCI, CCII and CCIII (B)
1029 SMA - putamen pathway. Boolean logic OR waypoint regions of interest gates are
1030 illustrated in blue; AND gates in green. M = Midline.

1031

1032 **Figure 3.** Correlation matrices for the MRI metrics investigated across the different
1033 WM pathways. Colour intensity and the size of the circles are proportional to the

1034 strength of the correlation. * $p < 0.05$, ** $p < 0.01$, *** $p < 0.001$. The absolute
1035 correlation coefficient is plotted. MPF values were highly correlated across tracts,
1036 whereas this was not true for the other metrics

1037

1038 **Figure 4. Mean ratings for drumming performance** according to the Trinity College
1039 London marking criteria for percussion (2016) as a function of group and time point.
1040 Patients improved their drumming performance significantly for the easy test pattern
1041 and controls for the medium difficult test pattern. * $p < 0.05$, ** $p < 0.01$, bootstrapping
1042 based on 1000 samples.

1043

1044 **Figure 5. MPF changes scores: PCA scree plot (A);** plot summarising how each
1045 variable is accounted for in every principal component - colour intensity and the size
1046 of the circles are proportional to the loading: PC1 loads on CCI, CCII, CCIII and right
1047 SMA-Putamen, while PC2 loads mostly on the left SMA-Putamen; the absolute
1048 correlation coefficient is plotted (B); correlation circle, interpreted as follows: 1)
1049 positively correlated variables are grouped together, 2) negatively correlated variables
1050 are positioned on opposite sides of the plot origin (opposite quadrants), 3) the distance
1051 between variables and the origin measures the quality of the variable on the factor
1052 map. Variables that are away from the origin are well represented on the factor map
1053 (C); Bar graph of the percentage change in MPF across the inspected tracts; Error
1054 bars represent the standard error; training was associated with a significantly greater
1055 change in MPF in CCII, CCIII, and right SMA-Putamen; * ($p < 0.05$), results corrected
1056 for multiple comparisons with FDR (D).

1057

1058 **Figure 6. TBSS analysis of baseline MPF values (A).** Light blue areas show a
1059 significant reduction of MPF in patients with HD compared to controls ($p < 0.05$, FWE
1060 corrected). The midbody of the CC was mostly found to be affected, which carries
1061 connections to the premotor, supplementary motor and motor areas of the brain.
1062 **Tracts showing significantly greater MPF changes in HD patients post-training**
1063 **as compared to controls (B).** Areas showing significant MPF reductions at baseline
1064 overlap with tracts showing significant changes post-training (i.e. CCII and CCIII).
1065
1066
1067
1068